A method to extend wavelength into middle-wavelength infrared based on InAsSb/(Al)GaSb interband transition quantum well infrared photodetector[*]

Xuan-Zhang Li(李炫璋)[1,2], Ling Sun(孙令)[1,2], Jin-Lei Lu(鲁金蕾)[1,2], Jie Liu(刘洁)[1,2], Chen Yue(岳琛)[1,2],
Li-Li Xie(谢莉莉)[3], Wen-Xin Wang(王文新)[1], Hong Chen(陈弘)[1,4], Hai-Qiang Jia(贾海强)[1,4], and Lu Wang(王禄)[1,†]

[1] Key Laboratory for Renewable Energy, Beijing Key Laboratory for New Energy Materials and Devices,
Beijing National Laboratory for Condensed Matter Physics, Institute of Physics, Chinese Academy of Sciences, Beijing 100190, China
[2] University of Chinese Academy of Sciences, Beijing 100049, China
[3] Detector Technology Laboratory, Beijing Institute of Space Mechanics & Electricity, Beijing 100076, China
[4] Songshan Lake Materials Laboratory, Dongguan 523808, China

We present a method to extend the operating wavelength of the interband transition quantum well photodetector from an extended short-wavelength infrared region to a middle-wavelength infrared region. In the modified InAsSb quantum well, GaSb is replaced with AlSb/AlGaSb, the valence band of the barrier material is lowered, the first restricted energy level is higher than the valence band of the barrier material, the energy band structure forms type-II structure. The photocurrent spectrum manifest that the fabricated photodetector exhibits a response range from 1.9 μm to 3.2 μm with two peaks at 2.18 μm and 3.03 μm at 78 K.

1. Introduction

Nowadays, middle wavelength infrared (MWIR) photodetectors have been widely studied in environmental monitoring,[1–3] and aerospace industry fields.[4,5] Especially, HgCdTe detectors have been deeply studied during the development of the MWIR photodetectors. However, the crystal growth of HgCdTe suffers the nonuniformity and size limitation of substrates, which limits the applications of IR FPAs.[6–10] From the viewpoint of producibility, the InAsSb material system is an ideal alternative material system for HgCdTe due to its superior electronic properties and growth stability,[11,12] its dielectric constant is low (≈ 11.5) and the room temperature self-diffusion coefficient is low ($\approx 5.2 \times 10^{-16}$ cm^2/s). The InAsSb material system can be applied in the nBn detectors,[13] pin detectors[14] and different low-dimensional-structure detectors.[15,16] Based on the InAsSb material system, the corresponding wavelength of the photodetectors can cover short wavelength infrared (SWIR) region and MWIR even long wavelength infrared (LWIR) regions.[17,18]

Recently, it has been reported that the photo-excited carriers in a low-dimensional semiconductor material can be effectively extracted from a p–n junction by inserting quantum wells into the depletion region of a p–n junction, the response spectrum can be extended, quantum efficiency can increase and the absorption efficiency in the

quantum wells (QWs) can be rather high, which can enhance the signal-to-noise ratio.[19–22] Based on those phenomena, researchers have fabricated three infrared interband transition quantum well detectors on different substrates, including GaAs-based InGaAs/GaAs QWs detectors,[23] InP-based InAs/InGaAs/InAlAs QWs detectors,[24] and GaSb-based lattice-matched GaSb/InAsSb QWs detectors.[25] All the detectors have successfully proved the effectiveness of utilizing interband transition of QWs as a new method of detecting IR spectra. The above results demonstrate the possibility to fabricate new type of MWIR interband band transition quantum well infrared photodetectors (IQWIPs) based on InAsSb heterostructures within a p–n junction.

To implement the innovative MWIR IQWIPs, a key step is extending the response wavelength from short wavelength to middle wavelength. However, there has been no report on the method to extend the wavelength of an IQWIP based on InAsSb hetero structures within a p–n junction so far. In this work, based on the InAsSb/GaSb lattice matched prototype detector, we apply a method to extend the wavelength of a GaSb-based IQWIP, the method of extending the response wavelength into MWIR is found and a MWIR photodetector based on InAsSb/AlSb/AlGaSb interband transition multiple quantum wells is successfully fabricated.

2. Experiment

In the photodetector based on InAsSb/GaSb multiple quantum wells, the energy level position in a quantum well is essential for designing an effective device. Hence the modification of the structure is focused on the energy band structure of InAsSb/GaSb quantum wells. The InAsSb/(Al)GaSb quantum-well energy band structures are firstly calculated under the framework of effective-mass approximation as shown in Fig. 1. After the theoretical analysis, two $InAs_{0.91}Sb_{0.09}$/GaSb QWs structures with different thicknesses of quantum wells and an InAsSb/AlSb/AlGaSb QW structure were grown in a V80 H solid source molecular beam epitaxy (MBE) system equipped with a valved arsenic and antimony cracker sources, a reflection high energy electron diffraction (RHEED) was equipped in MBE to monitor crystal growth quality. The $InAs_{0.91}Sb_{0.09}$/GaSb IR photodetector structures were started with growing a 300-nm-thick n-GaSb (4×10^{17} cm^{-3}) buffer layer to smooth the surface, then a 50-nm un-doped GaSb barrier layer, followed by 10-period $InAs_{0.91}Sb_{0.09}$ (10 nm or 15 nm)/GaSb (50 nm) MQWs, a 200-nm-thick p-GaSb (4×10^{17} cm^{-3}), 150-nm-thick p$^+$-GaSb (1×10^{18} cm^{-3}) and 5-nm-thick p$^+$-InAs (1×10^{18} cm^{-3}) as the contact layer, as shown in Fig. 2(a). The structure of the $InAs_{0.7}Sb_{0.3}$/AlSb/$Al_{0.3}Ga_{0.7}$Sb IR photodetector was embedded in the same p–n zone, but the un-doped zone began from a 40-nm un-doped $Al_{0.3}Ga_{0.7}$Sb barrier layer, followed by 10-period $InAs_{0.7}Sb_{0.3}$ (10 nm)/AlSb (10 nm)/$Al_{0.3}Ga_{0.7}$Sb (40 nm), as shown in Fig. 2(b). The growth temperature was 430 °C, and the growth rates depending on gallium, aluminum and indium beam flux were 5000 Å/h, 2143 Å/h and 2000 Å/h, respectively.
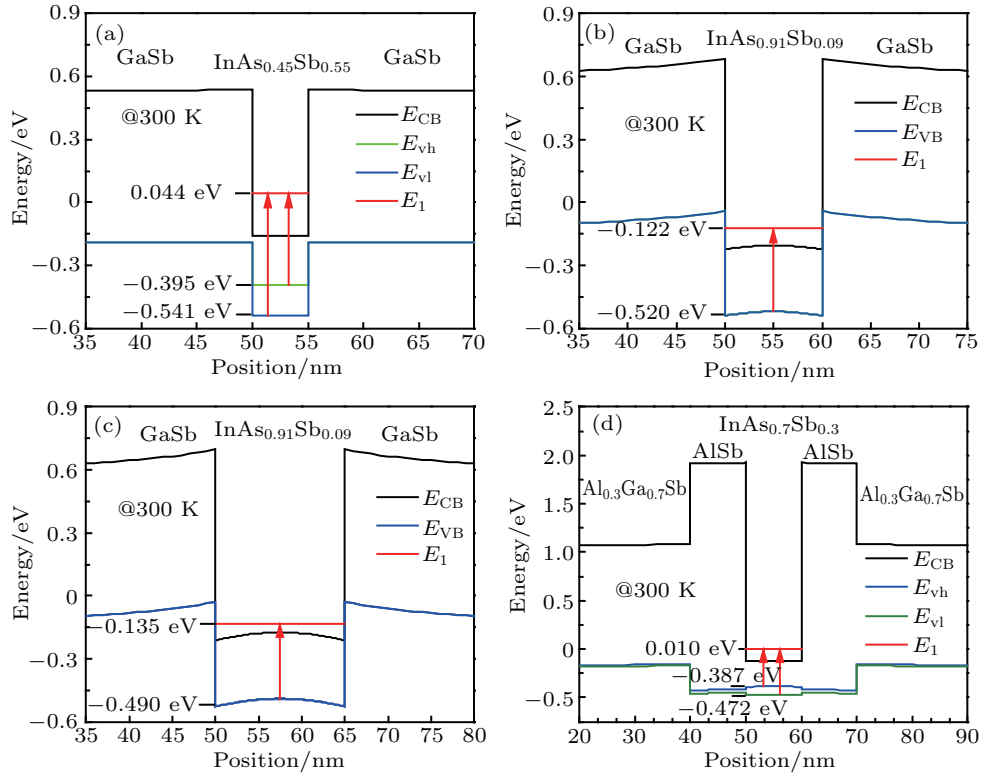
Fig. 1. Band structure of a single QW embedded in GaSb bulk at 300 K. The red arrows indicate the transition from the valence band of InAsSb (E_V) to the first excited state (E_1): (a) 5-nm-thick $InAs_{0.45}Sb_{0.55}$ QW, where the transition from the heavy hole valence band (E_{vh}) to the first excited state (E_1) of $InAs_{0.45}Sb_{0.55}$ is 0.44 eV, the response cut-off wavelength (λ_{off}) is 2.82 μm; (b) 10-nm-thick $InAs_{0.91}Sb_{0.09}$ QW, where the transition from the heavy hole valence band (E_{vh}) to the first excited state (E_1) is 0.39 eV ($\lambda_{off} = 3.16$ μm); (c) 15-nm-thick $InAs_{0.91}Sb_{0.09}$ QW, where the transition from the heavy hole valence band (E_{vh}) to the first excited state (E_1) is 0.35 eV ($\lambda_{off} = 3.54$ μm); (d) $InAs_{0.70}Sb_{0.30}$/AlSb/$Al_{0.30}Ga_{0.70}$Sb QW, where the transition from heavy hole valence band (E_{vh}) to E_1 is 0.39 eV ($\lambda_{off} = 3.16$ μm), the transition from light hole valence band (E_{vl}) at 300 K is 0.48 eV ($\lambda_{off} = 2.59$ μm).

The crystal quality was assessed using high resolution x-ray diffraction (XRD). After characterizing the crystal quality, the wafers were fabricated into a set of mesa-isolated photodetectors by photolithofraphy and wet etching. The fabricated device area is 1 mm^2. The electrodes of 20/100-nm Ti/Au were deposited onto the p-InAs in sequence by electron-beam evaporation. Then, 15/101/26/26/100-nm-thick Ni/Au/Ge/Ni/Au layers were deposited on the n-GaSb for an n-ohmic contact. The samples were loaded into a cryostat with a germanium (Ge) window for the test of photocurrent (PC) spectrum, the cryostat with a germanium (Ge) window provided a temperature controlled vacuum environment for the PC test, the PC spectrum was the typical normalized relative spectral response curve tested under zero bias voltage with a Bruker VERTEX 80 Fourier transform infrared spectrometer, the test wavelength range was from 1 μm to 6 μm. All the subsequent results can refer to the uncoated, unpassivated detectors.

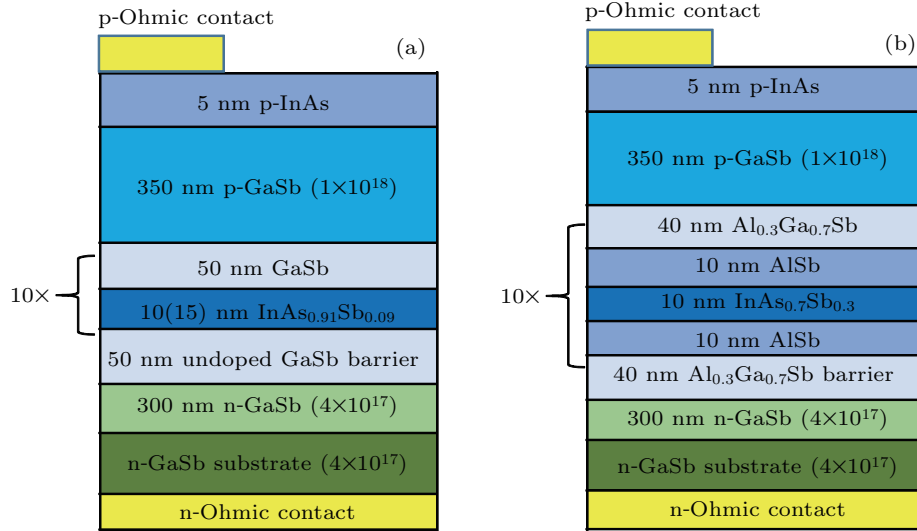**Fig. 2.** Schematic diagrams of (a) the InAs$_{0.91}$Sb$_{0.09}$/GaSb and (b) InAs$_{0.7}$Sb0.3/AlSb/Al$_{0.3}$Ga$_{0.7}$Sb quantum well IR photodetectors.

3. Result and discussion

As reported in Ref. [25], because of the quantum confinement modulation in the InAsSb/GaSb quantum well, the effective band gap was enlarged. The interband transition in the structure is from the valence band (E_{VB}) to the first excited state (E_1) of InAsSb QWs. The first effort to extend the response wavelength was increasing the composition of Sb in InAsSb, from 0.09 to 0.55. As shown in Fig. 1(a), the quantum well is a type-II structure, the transition from the heavy hole valence band (E_{vh}) to the first excited state (E_1) of InAs$_{0.45}$Sb$_{0.55}$ is 0.44 eV, the response cut-off wavelength (λ_{off}) is 2.82 μm, which is still in the SWIR region. In addition, the high incorporation of Sb in the InAs$_{0.45}$Sb$_{0.55}$ epitaxial layer introduces a lattice mismatch of about 3.2% with respect to the GaSb substrate, which will degrade the material quality and the performance of the photodetector.[26] Thus, only by increasing the incorporation of Sb in the InAs$_{1-x}$Sb$_x$ quantum well is unable to extend the wavelength from the eSWIR to the MWIR region.

The next effort to extend the response wavelength is broadened the width of the InAs$_{0.91}$Sb$_{0.09}$ quantum well from 5 nm to 10 nm (IQWIP-A) and 15 nm (IQWIP-B), respec-

tively, the thickness of a GaSb barrier is 50 nm. The energy band structures are shown in Figs. 1(b) and 1(c). After increasing the quantum well width, the valence of GaSb is higher than E_1, the quantum well structures of IQWIP-A and IQWIP-B both convert from type-II to type-III. The transition energy of the IQWIP-A and IQWIP-B are 0.39 eV (λ_{off} = 3.16 μm) and 0.35 eV (λ_{off} = 3.54 μm), respectively, both the absorption wavelengths shift from the SWIR to the MWIR region. Therefore, it is possible for the InAsSb/GaSb material system to cover the MWIR spectrum region theoretically, by increasing the width of well.

Then the structures were grown by MBE, which were characterized by XRD as shown in Figs. 3(a) and 3(b). The overall thickness of the quantum well structure per period is given by the following expression:

$$D = t_w + t_b = \lambda/(2\Delta\theta_p \cos\theta_B), \tag{1}$$

where t_w is the thickness of a quantum well, t_b is the thickness of a barrier, the $\Delta\theta_p$ determined from the angle between the satellite peaks and θ_B is the Bragg angle of the GaSb (004) diffraction.
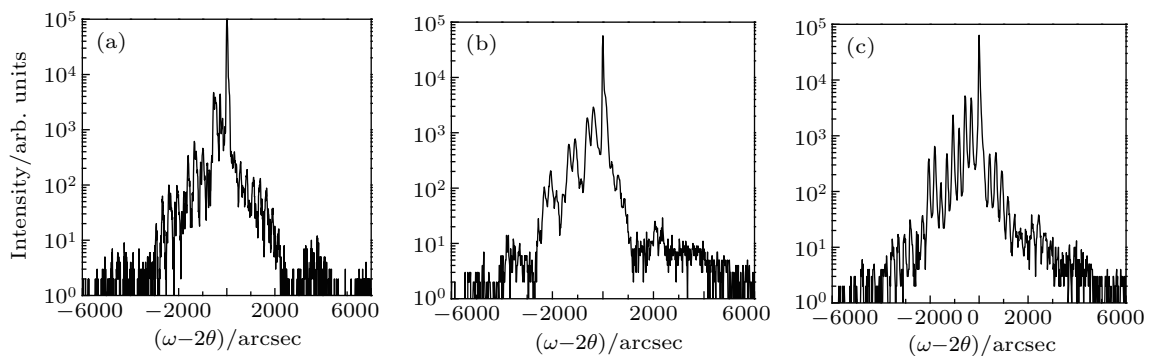

Fig. 3. X-ray diffraction pattern of InAs$_{0.91}$Sb$_{0.09}$/GaSb QWs and InAs$_{0.7}$Sb$_{0.3}$/AlSb/Al$_{0.3}$Ga$_{0.7}$Sb QWs: (a) the 10-nm InAs$_{0.91}$Sb$_{0.09}$ well in InAs$_{0.91}$Sb$_{0.09}$/GaSb QWs, (b) 15-nm InAs$_{0.91}$Sb$_{0.09}$ well in InAs$_{0.91}$Sb$_{0.09}$/GaSb QWs, (c) 10-nm InAs$_{0.7}$Sb$_{0.3}$ well in InAs$_{0.7}$Sb$_{0.3}$/AlSb/Al$_{0.3}$Ga$_{0.7}$Sb QWs.

The satellite peaks in the XRD curves show the quantum well periods of (a) 61 Å and (b) 67 Å, which coincide with the design value.

The photocurrent (PC) spectra of IQWIP-A and IQWIP-B are shown in Fig. 4(a). Compared with the spectrum of the device with the 5-nm-thick InAsSb quantum well, IQWIP-A and IQWIP-B have no response peak in the region from 1.6 μm to 4.0 μm at room temperature. Considering the impact to the signal-to-noise ratio from the dark current, the optical characterization was tested again at 78 K, but there was still no response signal from IQWIP-A and IQWIP-B. Compared the energy band structures of $InAs_{0.91}Sb_{0.09}$ (5 nm)/GaSb (50 nm) QW structure in Ref. [25], the structure is of type II, the main transition in this structure is from the E_{VB} of InAsSb to E_1, then the electron is extracted from the quantum well and a response current is formed, but the energy band structures of IQWIP-A and IQWIP-B are of type III, the transport mechanism is different from that of type II. The transition process of the type-III structure is that the electron leaps from the E_{VB} of InAsSb to E_1, because E_1 of InAsSb is lower than the valance band of GaSb, then the electron is not extracted from the quantum well but absorbed into the valance band of GaSb barrier and recombines with the hole finally, so no response current is generated. Thus, increasing the thickness of InAsSb well in the InAsSb/GaSb lattice matched quantum well is not available to extend the wavelength into the MWIR region, the structure of the photodetector should be of type II.

Hence, the QW structure was modified further, so that it gave us the structure of IQWIP-C. AlSb is approximately lattice-matched to GaSb, whereas has a wider band gap.[27] Using AlSb and the ternary alloy $Al_{0.3}Ga_{0.7}Sb$ as the barrier can raise the E_1 of InAsSb, so IQWIP-C replaces the GaSb barrier with $Al_{0.3}Ga_{0.7}Sb$ and inserting AlSb between $Al_{0.3}Ga_{0.7}Sb$ and InAsSb, the thicknesses of AlSb and $Al_{0.3}Ga_{0.7}Sb$ are 10 nm and 40 nm, respectively. Considering that the Al(Ga)Sb barrier would increase the band gap of the QW, we increased the well width to 10 nm to reduce the band gap of the QW, the molar fraction of Sb in InAsSb was 0.3. The structure of $InAs_{0.7}Sb_{0.3}/AlSb/Al_{0.3}Ga_{0.7}Sb$ was calculated within the framework of effective mass approximation.

As shown in Fig. 1(d), the energy band structure of the $InAs_{0.7}Sb_{0.3}/AlSb/Al_{0.3}Ga_{0.7}Sb$ quantum well is a type-II structure, the valence band of light hole is separated from that of heavy hole in the quantum well, the transition from heavy hole valence band (E_{vh}) to E_1 is 0.39 eV ($\lambda_{off} = 3.16$ μm) at 300 K, the transition from light hole valence band (E_{vl}) at 300 K is 0.48 eV ($\lambda_{off} = 2.59$ μm) at 300 K. The result shows that the IQWIP-C can get the response wavelength in the MWIR region.

The structure was grown and the crystal of the epitaxial layer was characterized by XRD, as shown in Fig. 3(c). From Eq. (1), the thickness of the QW structure per period in IQWP-C is 73 Å, which coincides with the design value.

Figure 4(b) shows the PC spectrum of IQWIP-C at 78 K, there are two peaks in the PC response curve. The first peak is around 2.287 μm, the second peak is around 3.026 μm. Contacted with the band structure of IQWP-C in Fig. 1(d), two peaks are corresponding to the transition from the $InAs_{0.7}Sb_{0.3}$ valence of light and heavy hole to E_1. The result demonstrates that the structure of IQWIP-C can extend the wavelength into the MWIR region and the position of E_1 higher than the valence of the barrier can make a response occur, which means that the type-II structure is necessary for the operatiion of the photodetector.
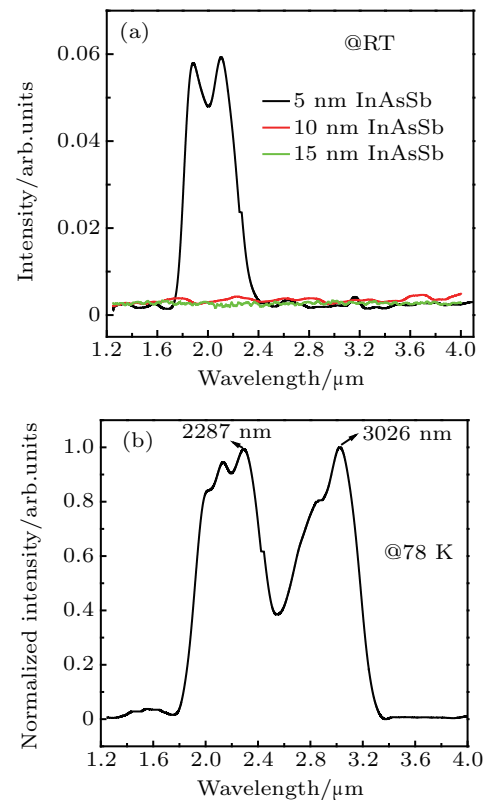

Fig. 4. Typical normalized relative photocurrent spectral response curves of (a) $InAs_{0.91}Sb_{0.09}$/GaSb QWs with different quantum wells: 5 nm, 10 nm (IQWP-A) and 15 nm (IQWP-B) under zero bias at room temperature; (b) IQWIP-C $InAs_{0.7}Sb_{0.3}/AlSb/Al_{0.3}Ga_{0.7}Sb$ QWs under zero bias at 78 K.

4. Conclusion

Through the theoretical design, growth, device fabrication, crystal and optical characterization, we have demonstrated a method to extend a wavelength from a short wavelength into a middle wavelength of InAsSb/(Al)GaSb quantum wells based on interband transition, with the wavelength peak at 3.026 μm, and we have drawn the following conclusion: type-II structure is necessary for operation of the photodetector. The results in this work provide a feasible way to extend the wavelength of the detector based on interband transition of InAsSb/Al(Ga)Sb quantum wells.

Acknowledgment

References

[1] Craig A P, Al-Saymari F, Jain M, Bainbridge A, Savich G R, Golding T, Krier A, Wicks G W and Marshall A R 2019 *Appl. Phys. Lett.* **114** 151107

[2] Hu W, Li Q, Chen X and Lu W 2019 *Acta Phys. Sin.* **68** 120701 (in Chinese)

[3] Letka V, Bainbridge A, Craig A P, Al-Saymari F and Marshall A R J 2019 *Opt. Express* **27** 23970

[4] Pavlov N and Zegrya G 2016 *J. Phys.: Confer. Ser.* **769** 012076

[5] Cardimona D A, Huang D H, Cowan V and Morath C 2011 *Infrared Phys. & Technol.* **54** 283

[6] Rogalski A 2011 *Infrared Phys. & Technol.* **54** 136

[7] Rogalski A 2010 *J. Mod. Opt.* **57** 1716

[8] Rogalski A 2009 *Acta Phys. Pol.* **116** 389

[9] Rogalski A, Antoszewski J and Faraone L 2009 *J. Appl. Phys.* **105** 091101

[10] Rogalski A 2003 *Prog. Quantum Electron.* **27** 59

[11] Zhang Y, Zhang Y, Guan M, Cui L, Wang C and Zeng Y 2013 *J. Appl. Phys.* **114** 111108

[12] Belenky G, Wang D, Lin Y, Donetsky D, Kipshidze G, Shterengas L, Westerfeld D, Sarney W L and Svensson Stefan P 2013 *Appl. Phys. Lett.* **102** 111108

[13] Maimon S and Wicks G W 2006 *Appl. Phys. Lett.* **89** 151109

[14] Tong J, Tobing L Y, Ni P and Zhang D H 2018 *Appl. Surf. Sci.* **427** 605

[15] Ariyawansa G, Reyner C J, Steenbergen E H, Duran J M, Reding J D, Scheihing J E, Bourassa H R, Liang B L and Huffaker D L 2016 *Appl. Phys. Lett.* **108** 022106

[16] Huang Y, Ryou J H, Dupuis R, D'costa V, Steenbergen E, Fan J, Zhang Y H, Petschke A, Mandl M and Chuang S L 2011 *J. Cryst. Growth* **314** 92

[17] Coderre W M and Woolley J C 1970 *Can. J. Phys.* **48** 463

[18] D'souza A, Robinson E, Ionescu A C, Okerlund D, De Lyon T J, Sharifi H, Roebuck M, Yap D, Rajavel R D, Dhar N, Wijewarnasuriya P S and Grein C 2012 *J. Electron. Mater.* **41** 2671

[19] Yang H, Ma Z, Jiang Y, Wu H, Zuo P, Zhao B, Jia H and Chen H 2017 *Sci. Rep.* **7** 43357

[20] Wu H, Ma Z, Jiang Y, Wang L, Yang H, Li Y, Zuo P, Jia H, Wang W, Zhou J, Liu W and Chen H 2016 *Chin. Phys. B* **25** 117803

[21] Sun Q, Wang L, Jiang Y, Ma Z, Wang W, Sun L, Wang W, Jia H, Zhou J and Chen H 2016 *Chin. Phys. Lett.* **33** 106801

[22] Wang W, Wang L, Jiang Y, Ma Z, Sun L, Liu J, Sun Q, Zhao B, Wang W, Liu W, Jia H and Chen H 2016 *Chin. Phys. B* **25** 097307

[23] Liu J, Wang L, Sun L, Wang W-Q, Wu H, Jiang Y, Ma Z, Wang W, Jia h and Chen H 2018 *Acta Phys. Sin.* **67** 128101 (in Chinese)

[24] Liu J, Lu J, Yue C, Li X, Chen H and Wang L 2019 *Appl. Phys. Express* **12** 032005

[25] Sun L, Wang L, Lu J L, Liu J, Fang J, Xie L L, Hao Z B, Jia H Q, Wang W X and Chen H 2018 *Chin. Phys. B* **27** 047209

[26] Sun Q L, Wang L, Wang W Q, Sun L, Li M C, Wang W X, Jia H Q, Zhou J M and Chen H 2015 *Chin. Phys. Lett.* **32** 106801

[27] Mohammedy F M and Deen M J 2009 *J. Mater. Sci.: Mater. Electron.* **20** 1039